Sigma-1 Receptor Imaging in the Brain

Kuzhuppilly Ramakrishnan, Nisha

Sigma-1 receptor binding in the aging rat brain: A microPET study with ^{11}C-SA4503

Nisha K. Ramakrishnan [1], Anniek K.D. Visser [1], Anna A. Rybczynska [1], Csaba J. Nyakas [2], Chantal Kwizera [1], Jurgen W.A. Sijbesma [1], Philip H. Elsinga [1], Kiichi Ishiwata [3], Rudi A.J.O. Dierckx [1], Aren van Waarde [1]

[1] University of Groningen, University Medical Center Groningen, Department of Nuclear Medicine and Molecular Imaging, Groningen, The Netherlands
[2] Brain Physiology Research Unit, Semmelweis University, Budapest, Hungary
[3] Tokyo Metropolitan Institute of Gerontology, Tokyo, Japan

3

Submitted

ABSTRACT

Sigma-1 receptor agonists modulate the release of several neurotransmitters and intracellular calcium signaling. It has been proposed that their binding sites are upregulated in the aging brain to compensate for age-related losses of activity in other neurotransmitter systems. In this study we investigated sigma-1 receptors in the living rat brain to test this hypothesis. Sigma-1 receptors in young (1.5 and 3 months) and aged (18, 24 and 32months) Wistar Hannover rats were visualized using ^{11}C-SA4503. Time-dependent tracer uptake was measured using a microPET camera, and tracer-kinetic models were fitted to this data, using metabolite-corrected plasma radioactivity and uncorrected whole blood radioactivity as input function. Aged rats metabolised ^{11}C-SA4503 to a lesser extent than young rats. Logan graphical analysis and a 2-tissue compartment model (2-TCM) fit revealed that total distribution volume (V_T), binding potential (BP_{ND}) and partition coefficient (K_1/k_2) of the tracer were significantly reduced with aging. BP_{ND} was reduced particularly in thalamus, hypothalamus, midbrain, pons and medulla. The PET data did not provide support for any upregulation of sigma-1 receptors in healthy aging. Sigma-1 receptor losses may be associated with endocrine changes in aged rats and greater sensitivity of neurons to apoptotic signals.

Keywords: Cutamesine, Imaging, Kinetic analysis, Wistar-Hannover rat.

INTRODUCTION

Sigma-1 receptors are widely distributed in the brain and are strongly expressed in neurons and glia *(1)*. They are involved in cellular differentiation, neuroplasticity, neurogenesis, neuroprotection and cognition *(1, 2, 3, 4, 5)*. Sigma-1 receptors are ligand-regulated molecular chaperones in the endoplasmic reticulum and play a modulatory role in intracellular calcium signaling *(6)*. Upon activation, sigma-1 receptors translocate from the endoplasmic reticulum to the plasma membrane to modulate the activity of ion channels and regulate neurotransmitter release *(6)*. Sigma ligands modify the extracellular concentration of dopamine in rat brain *(7, 8, 9)* and sigma-1 agonists cause dose-dependent increases in the extracellular levels of acetylcholine *(10, 11, 12, 13, 14)* and glutamate *(15, 16, 17)*.

The density of dopaminergic, cholinergic and glutamatergic receptors is known to decline with age both in the rodent *(18, 19, 20)* and human *(21, 22, 23)* brain. Levels of neuroactive steroids such as progesterone and dehydroepiandrosterone, which are considered as endogenous ligands for sigma receptors, are also reduced during aging *(24, 25)*.

It has been proposed *(26, 27, 28)* that increased sigma-1 receptor signaling in the aging brain might compensate for the decline of the function of various neurotransmitter systems and for the loss of endogenous neurosteroids. This hypothesis is based on the following findings: First, dopamine D2 receptor density in the striatum of Fischer-344 x Brown Norway rats is reduced (by 36 to 41%) at old age in contrast to total sigma receptor density (sigma-1 plus sigma-2) which is significantly increased (by 35 to 42%) *(26)*. Second, the binding potentials (B_{max}/K_d ratios) of the sigma-1 ligand [^{3}H]pentazocine and the non-subtype-selective sigma ligand [^{3}H]DTG are increased in the brain of Fisher-344 rats at old age (24-mo), although both the number of binding sites (B_{max}) and dissociation constants (K_d values) of the two ligands are elevated *(27)*. Third, an age-related 60 to 110% increase in the binding potential of ^{11}C-SA4503 has been detected in the monkey brain with PET *(28)*.

However, data reported in other publications conflict with these findings. While in the brains of Fischer 344-related rats, sigma-1 receptor numbers were found to be either increased or unaffected by aging *(26, 27, 29)*, in Sprague-Dawley rats age-related decreases of receptor number and affinity were noted *(30, 31)*. Similarly, while aging cynomolgus monkeys showed significant increases of BP_{ND} of ^{11}C-SA4503 in cortical regions, hippocampus, striatum, thalamus and cerebellum *(28)*, ^{11}C-SA4503 scans in aging humans indicated decreases of BP_{ND} in cerebellum, hippocampus, temporal and occipital cortices and slight increases in the putamen and head of the caudate nucleus *(32)*. Sigma-1 receptor populations may thus be differently affected in different brain regions, rodent strains and primate species.

Published data for sigma receptor expression in the aging rat brain were acquired using *in vitro* binding assays of striatum *(26)* or whole brain *(27, 29, 30, 31)* homogenates. In the current study, we investigated the effect of aging on

sigma-1 receptor binding potential in the brain of living rats, using ^{11}C-SA4503 and microPET. Regional differences could thus be assessed in the intact organism.

We aimed to test the hypothesis that increases of sigma-1 receptor signaling compensate for age-related losses of function of other neurotransmitter systems. Based on this hypothesis and on PET findings in non-human primates *(28)* we expected to observe increases of sigma-1 receptor expression at advanced age.

MATERIALS AND METHODS

Radioligand

The ligand 1-[2-(3,4-dimethoxyphenethyl)]-4-(3-phenylpropyl)piperazine (^{11}C-SA4503) was prepared by reaction of ^{11}C-methyl iodide with 4-O-demethyl SA4503, according to a published method *(33)*. The decay corrected radiochemical yield was ~ 24%, the specific radioactivity was > 100 TBq/mmol at the moment of injection and radiochemical purity > 98%. The ^{11}C-SA4503 solution had a pH of 6.0 to 7.0.

Animals

Male Wistar Hannover rats were obtained from Harlan (The Netherlands) and Semmelweis University Budapest. The age groups studied were 1.5 (n=9), 3 (n=10), 18 (n=5), 24 (n=4) and 32 (n=5) months. About 40% of the older rats were found to have pituitary tumors *(34)*. The microPET data of these animals were not included in the current study, but their blood samples provided some of the data for metabolite analysis. The rats were housed in Macrolon cages on a layer of wood shavings at 21 ± 2 °C and a fixed 12-hour light-dark regime (lights on at 7:00 a.m.). Food (standard laboratory chow, RMH-B, Hope Farms, The Netherlands) and water were available *ad libitum*. After arrival the rats were allowed to acclimatize for at least seven days. The protocol was approved by The Institutional Animal Care and Use Committee of the University of Groningen. The experiments were performed by licensed investigators in compliance with the Law on Animal Experiments of The Netherlands.

Arterial blood sampling

Before microPET scanning, rats were anesthetized with isoflurane in medicinal air (5% for induction and 2% for maintenance). An incision was made parallel to the femoral artery. The femoral artery was separated from the femoral vein and temporarily ligated to prevent leakage of blood. A small incision was made in the artery and a cannula was inserted (0.8 mm outer, 0.4 mm inner diameter). The cannula was secured to the artery with a suture and attached to a syringe filled with heparinized saline.

From each rat, fifteen arterial blood samples (volume 0.1 to 0.15 ml) were collected at 0.25, 0.5, 0.75, 1, 1.25, 1.5, 2.0, 3, 5, 7.5, 10, 15, 30, 60 and 90 minutes

after ^{11}C-SA4503 injection. 25 µl of whole blood was reserved and plasma was obtained from the remaining blood by centrifugation (5 min in Eppendorf-type centrifuge at 13,000 rpm). Radioactivity in the whole blood and plasma samples (25 µl) was determined using a calibrated gamma counter (CompuGamma CS 1282, LKB-Wallac, Turku, Finland)

In separate groups of rats, larger volumes of blood ranging from 0.4 to 1.6 ml were collected at 5, 10, 20, 40 and 60 min and a metabolite analysis was performed using a published method *(35)*. Briefly, plasma was obtained by centrifugation (2 min in Eppendorf-type centrifuge at 13,000 rpm) and de-proteinized using one third the volume of 20% trichloroacetic acid in acetonitrile. The mixture was centrifuged for 2 min at 13,000 rpm and the supernatant injected in a reversed-phase HPLC system to separate the parent tracer from its metabolites (MicroBondapak C18 column, 7.8 x 300 mm, mobile phase acetonitrile/50 mM sodium acetate pH 7.2, 1/1, v/v, flow rate 3 mL/min). The eluate was collected in 30 s fractions for 15 min and radioactivity in the samples was counted. The results were expressed as the percentage of total plasma radioactivity representing parent tracer.

Scanning

Two rats were scanned simultaneously in each scan session, using a Siemens/ Concorde microPET camera (Focus 220). They were placed in the camera in transaxial position with their heads and neck in the field of view. Body temperature of the animals was maintained with heating mats and electronic temperature controllers. Circulation and respiration could be monitored with the BioVet system (M2M Imaging, Cleveland, OH). First, a transmission scan of 515 s with a Co-57 point source was obtained for attenuation and scatter correction of 511 keV photons by tissue. Subsequently, the first rat was injected through the penile vein with ^{11}C-SA4503 (31±16 MBq, volume < 1 ml). This dose of [^{11}C]SA4503 results in maximally 5.0 to 7.5% sigma-1 receptor occupancy throughout the rat brain, whereas blocking studies using either non-radioactive cutamesine or donepezil have indicated that nonspecific binding of the tracer is between 20% and 25% of total uptake of radioactivity in all studied brain regions *(36)*. The emission scan was started with tracer injection of the first rat; whereas the second rat was injected a few minutes later. A list-mode protocol was used with 90 min acquisition time (analysis performed for first 74 min from tracer injection). The list-mode data of the emission scans were reframed into a dynamic sequence of 8x30s, 3x60s, 2x120s, 2x180s, 3x300s, 3x600s, 1x720s, 1x960s frames. The data were reconstructed per time frame employing an iterative reconstruction algorithm (ordered subsets expectation maximization, OSEM2D with Fourier rebinning, 4 iterations and 16 subsets). The final datasets consisted of 95 slices with a slice thickness of 0.8 mm, and an in-plane image matrix of 128 x 128 pixels. Voxel size was 0.5 x 0.5 x 0.8 mm. The linear resolution at the center of the field-of-view was about 1.5 mm. Data sets were fully corrected for decay, random coincidences, scatter and attenuation.

Data analysis

Using Inveon Research Workplace (Siemens), three-dimensional regions of interest (ROIs) were drawn on a MRI template of rat brain *(37)*, both over the whole brain and individual brain regions (bulbus, cortex, striatum, thalamus, hypothalamus, amygdala, midbrain, pons + medulla and cerebellum). PET images were co-registered with the MRI template and the regions of interest transferred from MRI to PET. Time-activity curves (TACs) were obtained for each of these regions. The results were expressed as dimensionless standardized uptake values (SUVs): [tissue activity concentration (MBq/g) × body weight (g) / injected dose (MBq)], assuming a specific gravity of 1 g/mL for brain tissue and blood plasma.

Kinetic analysis was performed by fitting a two-tissue compartment model (2-TCM) to the dynamic PET data using metabolite corrected arterial plasma radioactivity as input function. The plasma TAC of each animal was corrected for metabolites using an exponential function obtained from the average metabolite curve of the rats from the same group. Uncorrected whole blood data was used to estimate the contribution of radioactivity in blood to the measured brain radioactivity. Where plasma or whole blood data was not available, an age-matched group average corrected for injected dose and weight of individual animal was used as input. Software routines for MatLab 7 (The MathWorks, Natick, MA), written by Antoon T.M. Willemsen (University Medical Center Groningen), were used for curve fitting. The cerebral blood volume was fixed at 3.6% *(38)* and the rate constants K_1 (from arterial plasma to tissue), k_2 (from tissue to arterial plasma), k_3 (from free to bound compartment in tissue), and k_4 (from bound to free compartment in tissue) were estimated from the curve fit. Partition coefficient (V_{ND}) was calculated as K_1/k_2, non-displaceable binding potential (BP_{ND}) was calculated as k_3/k_4 and total distribution volume (V_T) was calculated as K_1/k_2 * (1+ k_3/k_4). V_{ND} obtained for the whole brain was fixed for each individual rat during the second phase of modelling for individual brain regions. Additionally, Logan graphical analysis was used to obtain cerebral distribution volume (V_{Logan}). The Logan fit was started at 20 min and the parameter for cerebral blood volume was fixed at 3.6%. V_{Logan} of the tracer was estimated from the curve fit. The binding potential for individual brain regions was also obtained from the V_{Logan} as BP_{Logan} = (V_{Logan} / V_{ND}) - 1, where V_{ND} was obtained from the whole brain of each individual rat using 2-TCM.

Biodistribution

After the scanning period, the animals were terminated under deep anesthesia by extirpation of the heart. Blood was collected, and plasma and a cell fraction were obtained from the blood sample by short centrifugation (10 min at 13,000 rpm). Several tissues (see Table 1) were excised and weighed. Radioactivity in tissue samples and in a sample of the injected tracer solution (infusate) was measured using a gamma counter with automatic decay correction. The results were expressed both as SUV and a ratio (SUV tissue/SUV plasma).

Statistics

All results are expressed as mean ± SEM. Differences between groups were examined using 1-way ANOVA (for area under the curves and whole brain 2-TCM parameters), 2-way ANOVA (biodistribution, brain and periphery analyzed separately) or repeated measures 2-way ANOVA (metabolite analysis and TACs), followed by a post hoc Bonferroni test, where applicable. A P value < 0.05 was considered statistically significant. Correlations were assessed using Pearson correlation coefficient (r) and considered strong when r^2 was at least 0.7.

RESULTS

PET images

In young rats (1.5 and 3 months) the highest tracer uptake was seen in the pons and medulla, followed by midbrain, thalamus and hypothalamus. Lower uptake was seen in cortex, striatum, hippocampus, bulbus, amygdala and cerebellum. In older rats (18, 24 and 32 months), regional differences were less obvious (Figure 1).

Tracer kinetics in plasma

Metabolite analysis was not performed in the 24 month old rats due to difficulty obtaining a sufficient number of rats; the information from 32 month old rats was used for their metabolite correction. Additionally, since pituitary tumor did not affect the metabolite formation[34], metabolism data from rats with pituitary tumor (1 rat aged 18 months and 3 rats aged 32 months) were included. While only about 30% of the parent tracer remained unchanged at 60 min in the 1.5 month old rats, nearly 60% was unchanged in the 32 month old rats, indicating possible impairment in liver and kidney function (Figure 2). All groups were significantly different (P < 0.001 to 0.05) from other groups in at least one time point.

Kinetics of radioactivity in plasma after metabolite correction is shown in Figure 3. While clearance was rapid in all age groups, the area under the curve (AUC) for 32-month-old rats was significantly higher (P < 0.001) than for other age groups. The rats aged 18 and 24 months also had significantly higher (P < 0.001) AUC than the young rats of 1.5 and 3 months.

Tracer kinetics in brain

Tracer uptake was rapid, a peak at <5 min being followed by a slow washout (Figure 4A). Significant differences between various age groups were observed in the TACs; 1.5 vs. 18 months, first 5 minutes; 1.5 vs. 32 months, first 22 minutes; 3 vs. 32 months, first 14 minutes; 24 vs. 32 months, first 4 minutes. AUC for the whole brain increased with age and reached significance (P < 0.01) between the youngest and oldest group (Figure 4B). The youngest age group showed greater regional differences in TACs than the oldest group (Figure 4C).

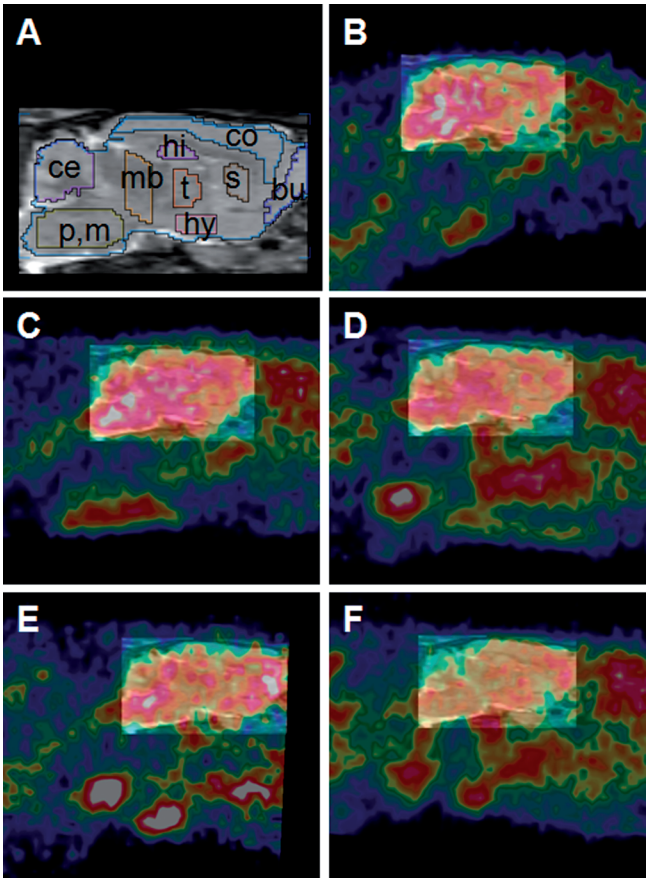

Figure 1. *MicroPET images of rat brain (sagittal view superimposed on MRI template, 22- to 74-min-frames summed, about 1.6 mm from the midline). A) MRI template, B) 1.5-months-old, C) 3-months- old, D) 18-months-old, E) 24-months-old and F) 32-months-old rats.*

Kinetic analysis

Using metabolite corrected plasma radioactivity from arterial blood samples, and uncorrected whole blood samples as input function, 2-TCM was fitted to ROIs drawn around whole brain. Tracer V_T significantly reduced with aging (Figure 5A). All three older age groups had significantly lower V_T compared to both younger groups. BP_{ND} also tended to decline with age (Figure 5B), this tendency reaching significance only between the 1.5-months and 18- or 32-months groups. Additionally, there was a reduction in K_1/k_2 with age (Figure 5C) which reached significance between the 3-months-old rats and the two oldest groups (24 and 32 months).

In the second phase of modeling, individual regions within the brain were analyzed using 2-TCM wherein the K_1/k_2 obtained from the whole brain was fixed for each individual rat. Due to similarities in the whole brain kinetic analysis

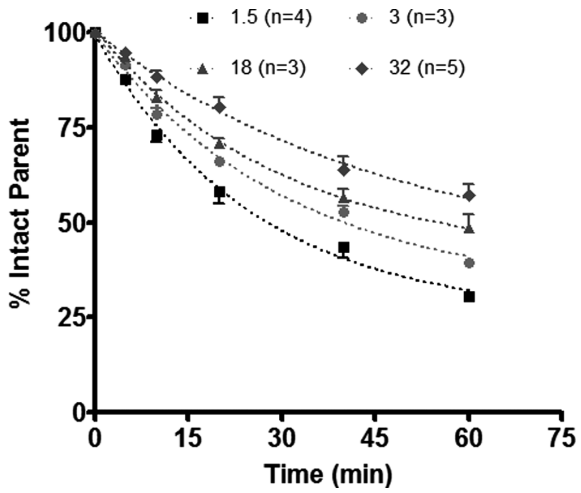

Figure 2. *Effect of aging on tracer metabolism (mean ± SEM).*

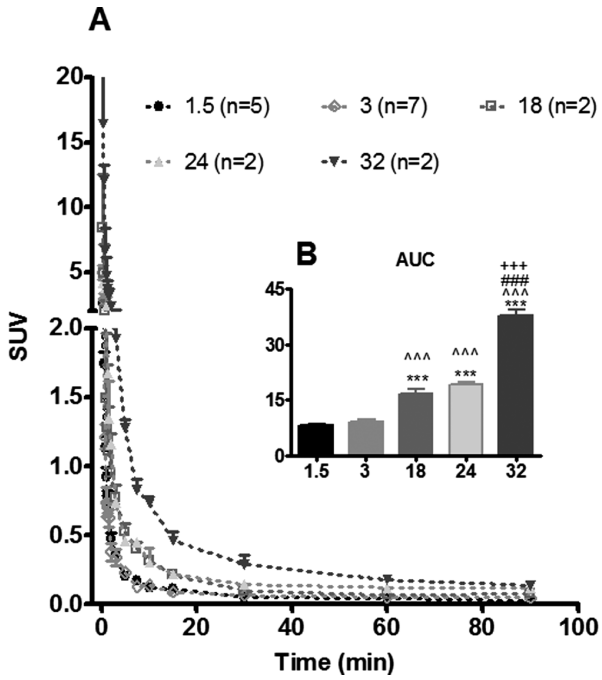

Figure 3. *Metabolite-corrected tracer kinetics in plasma. A) TACs for different age groups. B) AUC. * indicates comparison with 1.5-months-old, ^ with 3-months-old, # with 18-months-old and + with 24-months-old rats. *** indicates P < 0.001.*

results, the rats aged 1.5 and 3 months were combined as a "young" group while the rats aged 18, 24 and 32 months were combined to form an "aged" group in order to increase the power of analysis while comparing large numbers of regions. As was seen with the whole brain, all regions examined showed a highly significant reduction in V_T in the aged group (Figure 6A). Changes in BP_{ND} were not

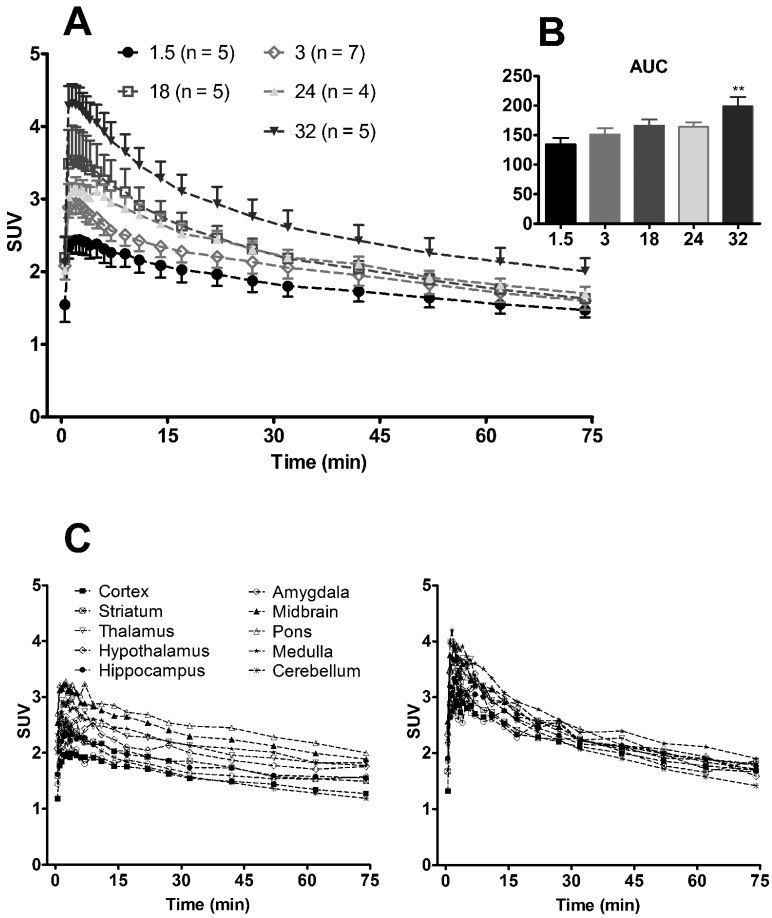

Figure 4. *Cerebral kinetics of ^{11}C-SA4503. Whole brain TACs (A) and AUCs (B) for the different age groups. * indicates comparison with 1.5-months-old rats, ** indicates P < 0.01. C) TACs for individual brain regions in young (left) and old (right) rats.*

as uniform: the reduction in bulbus, cortex and cerebellum were not significant (Figure 6B).

V_T and V_{Logan} for whole brain were strongly correlated ($r^2 = 0.99$, $P < 0.0001$) with V_{Logan} showing a slight underestimation of about 5% (see Supplementary Information). BP_{Logan} obtained from V_{Logan} for individual brain regions was also closely correlated with BP_{ND} ($r^2 = 0.95$, $P < 0.0001$), BP_{Logan} having an underestimation of about 11% (see Supplementary Information).

Biodistribution

Biodistribution data for brain and peripheral organs are listed in **Table 1.** Aged rats showed a significantly lower SUV in brain regions other than cerebellum or

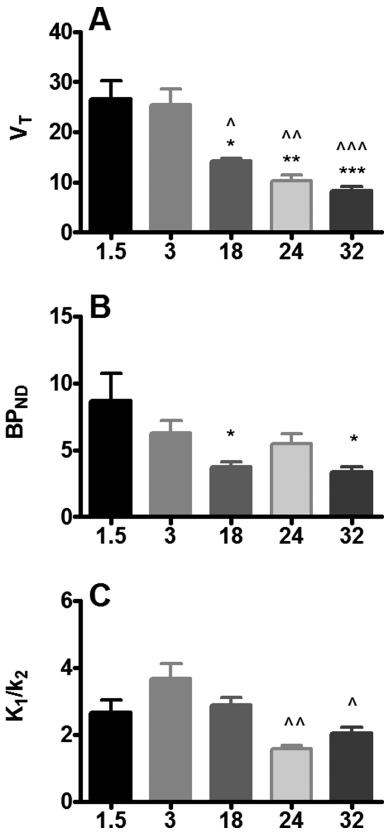

Figure 5. *2-TCM data of ^{11}C-SA4503 in different age groups: whole brain V_T (A), BP_{ND} (B), Partition coefficient (C). * indicates comparison with 1.5-months-old and ^ with 3-months-old. * P < 0.05, ** P < 0.01, *** P < 0.001.*

cortex, and a significantly higher SUV in spleen, submandibular gland and urine. However, since plasma SUV was significantly higher in aged rats (t-test: $P < 0.0001$), tissue-to-plasma ratio is a better measure of differences between groups. Tissue-to-plasma ratio in cerebellum and rest of the brain was significantly lower in aged rats, while cortex was not significantly different. Among peripheral tissues, kidney and liver had a significantly ($P < 0.001$) lower tissue-to-plasma ratio in aged rats.

DISCUSSION

The hypothesis of an age-related upregulation of sigma-1 receptors was not confirmed by our data. A reduced regional variability of tracer uptake was noticed in aged brains. While some brain regions appeared to be unaffected, most regions showed reduced uptake. Although average brain TACs were higher in old animals, plasma TACs were also higher resulting in a reduction in V_T with aging. Tracer-kinetic modeling proved essential as both the formation of radioactive

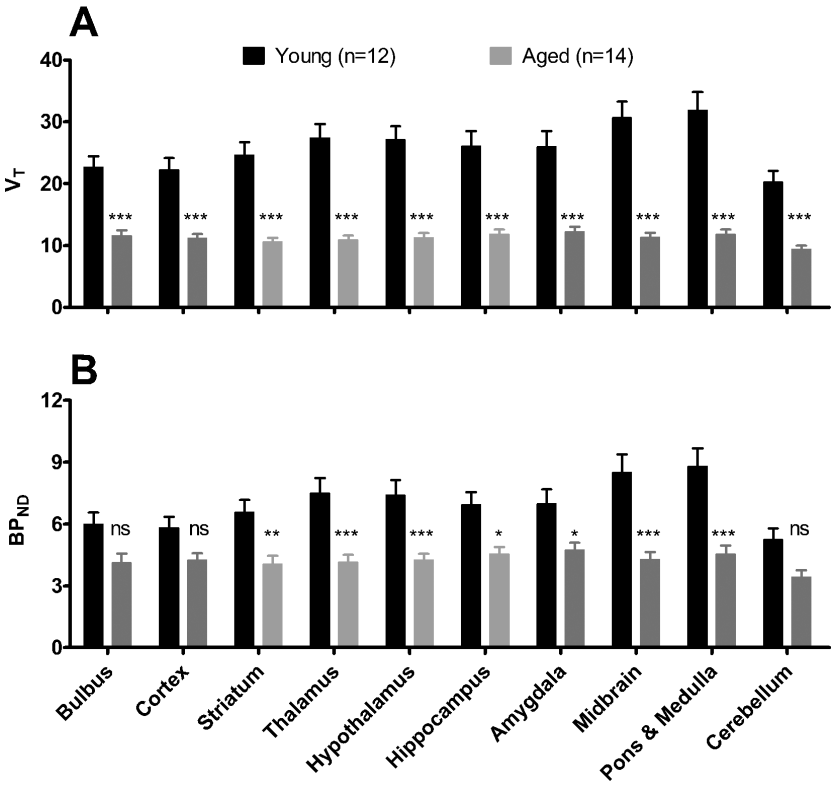

Figure 6. *2-TCM data of ^{11}C-SA4503 in brain regions. Ages 1.5 and 3 months were combined to form the young group and ages 18, 24 and 32 were combined to form the aged group. A) V_T, B) BP_{ND}, * P < 0.05, ** P < 0.01, *** P < 0.001.*

metabolites and plasma levels of radioactivity are influenced by aging. Considering only raw uptake (SUV values) could lead to misleading conclusions. Higher brain and plasma TACs in old animals could be related to the fact that aged rats weigh more than young ones and SUV measures tend to positively correlate with animal weight for most radiotracers. In addition, aged rats may show reduced liver and kidney function, resulting in slower tracer clearance.

The age-dependent reduction in whole brain V_T was found to be related to a reduction in both K_1/k_2 and BP_{ND}, suggesting changes of flow or blood-brain barrier permeability as well as reductions in the numbers and/or affinities of sigma-1 receptors with aging. The greatest decreases of binding were noted in thalamus, hypothalamus, midbrain, pons and medulla, i.e. regions associated with sleep, hormonal control, fear, posture, and autonomic function.

Our microPET data confirm the age-related decreases of receptor number and affinity which were measured with *in vitro* assays in aged Sprague-Dawley rats *(30, 31)*, but they are at variance with the increases reported in the Fischer 344

Table 1. Biodistribution of ^{11}C-SA4503 in brain and peripheral organs of young (1.5- and 3-months-old) and aged (18-, 24-, 32-months-old) rats. Data were acquired 90 min after intravenous radioligand injection.

	SUV			T/P ratio		
Tissue	**Young (n=16)**	**Aged (n=13)**	***P#***	**Young (n=16)**	**Aged (n=13)**	***P#***
Cerebellum	1.31 ± 0.09	1.33 ± 0.10	ns	12.70 ± 1.37	8.23 ± 1.00	< 0.05
Cerebral cortex	1.30 ± 0.08	1.56 ± 0.11	ns	12.43 ± 1.06	9.66 ± 1.11	ns
Rest brain	1.75 ± 0.10	1.36 ± 0.09	< 0.05	16.79 ± 1.52	8.45 ± 0.98	<0.001
Adipose tissue	0.47 ± 0.06	0.28 ± 0.06	ns	4.40 ± 0.56	1.66 ± 0.36	ns
Bladder	1.30 ± 0.20	2.34 ± 0.73	ns	13.04 ± 2.63	14.67 ± 5.14	ns
Bone	0.46 ± 0.05	0.43 ± 0.05	ns	4.19 ± 0.49	2.58 ± 0.31	ns
Bone marrow	2.29 ± 0.91	3.15 ± 0.73	ns	20.97 ± 8.38	17.67 ± 3.57	ns
Heart	0.36 ± 0.03	0.65 ± 0.04	ns	3.51 ± 0.44	3.92 ± 0.39	ns
Large intestine	1.91 ± 0.10	2.20 ± 0.16	ns	18.17 ± 1.53	13.51 ± 1.55	ns
Small intestine	2.29 ± 0.22	3.18 ± 0.26	ns	22.08 ± 2.96	19.49 ± 2.26	ns
Kidney	4.40 ± 0.23	3.50 ± 0.21	ns	42.00 ± 3.47	21.30 ± 1.89	<0.001
Liver	9.30 ± 0.39	10.78 ± 0.47	ns	87.37 ± 5.45	65.30 ± 5.37	<0.001
Lung	2.07 ± 0.11	2.24 ± 0.16	ns	19.69 ± 1.69	13.61 ± 1.38	ns
Muscle	0.17 ± 0.02	0.35 ± 0.06	ns	1.76 ± 0.27	2.13 ± 0.43	ns
Pancreas	5.18 ± 0.51	5.63 ± 0.59	ns	48.46 ± 5.86	34.75 ± 4.99	ns
Plasma	0.11 ± 0.01	0.17 ± 0.01	ns	1.00	1.00	ns
Red blood cells	0.06 ± 0.01	0.09 ± 0.01	ns	0.63 ± 0.07	0.50 ± 0.06	ns
Spleen	2.47 ± 0.17	4.45 ± 0.30	<0.01	23.52 ± 2.11	27.28 ± 2.81	ns
Submandibular gland	3.29 ± 0.25	5.98 ± 0.59	<0.001	30.82 ± 2.72	36.20 ± 4.58	ns
Urine	1.58 ± 0.28	3.32 ± 1.22	< 0.05	14.51 ± 2.67	21.33 ± 8.50	ns

strain *(26, 27, 29)*. Since Sprague-Dawley rats resemble our own Wistar Hannover rats quite closely in contrast to Fischer 344 rats, the discrepancies reported in the literature may indicate the presence of strain differences.

Reductions in K_1/k_2 are likely to be due to hypoperfusion caused by a decline in microvascular structures *(39)* rather than a reduction in permeability, as permeability across the blood brain barrier generally increases with aging *(40)*. Since BP_{ND} reflects B_{max}/K_d, either a reduction in receptor numbers or affinity of the tracer to the receptors could reduce this parameter. In a population-based approach, where the pharmacokinetics of ^{11}C-SA4503 was examined, we did not observe any reduction of K_d with aging (Chapter 9), suggesting that sigma-1 receptor density rather than affinity to ^{11}C-SA4503 is reduced in old rats.

Surprisingly, our rat data on sigma-1 receptor density resemble the age-related regional decreases observed in human brain *(32)* more closely than PET data on cynomolgus monkeys which indicated regional increases *(28)*. Reduced sigma-1 receptor binding in the human cortex could be one of the reasons for cognitive impairment in normal aging.

Regional changes in aging rats (binding particularly decreased in thalamus, hypothalamus, midbrain, pons and medulla, smaller declines in hippocampus, amygdala and striatum, Fig. 6) suggest that sigma receptor losses in aging rodents are related to endocrine changes and impaired autonomic functions in addition to impaired cognition. Sigma-1 receptor losses could also be associated with reduced viability of neurons and greater sensitivity to apoptotic signals *(41)*.

In conclusion, our microPET study provides evidence of a decrease of sigma-1 receptor numbers in the aging rodent brain contrary to our initial hypotheses. Tracer binding potential was particularly reduced in (hypo)thalamus, midbrain, pons, and medulla (less strikingly also in hippocampus, amygdala and, striatum). A global reduction in tracer partition coefficient was noted which may reflect an age-related decline in microvascular structures.

DISCLOSURE/CONFLICT OF INTEREST

There are no conflicts of interest to report concerning this paper.

SUPPLEMENTARY MATERIALS

Supplementary materials are available.

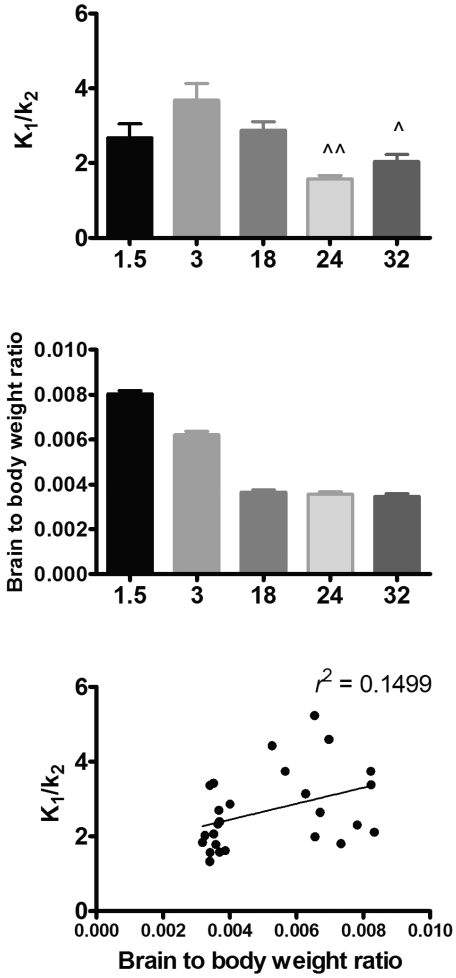

Supplementary Figure 1. *Tracer V_{ND} (from 2-TCM fit), brain-to-body weight ratio and (lack of) correlation of these parameters in our aging study population.*

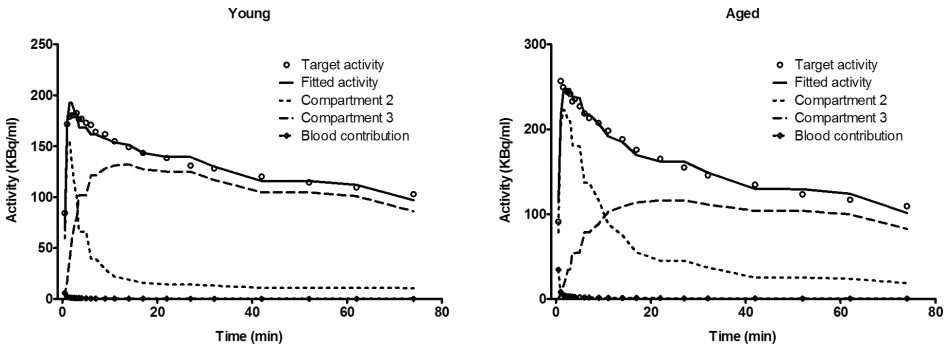

Supplementary Figure 2. *Representative examples of [^{11}C]SA4503 TAC in rat brain and the corresponding 2TCM fit. Left panel: young, right panel: aged animals.*

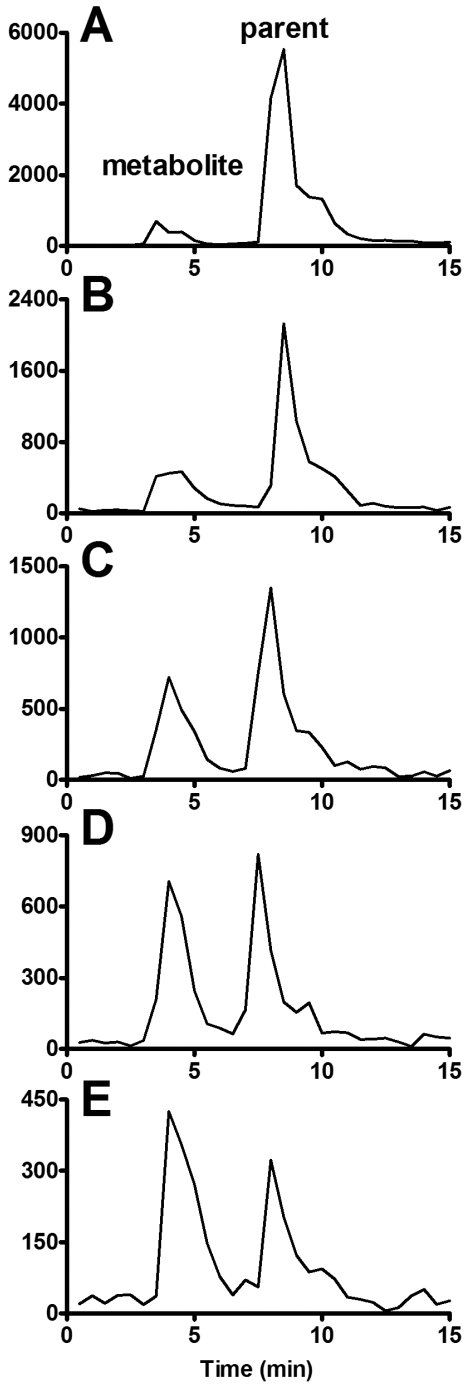

Supplementary Figure 3. *Representative HPLC chromatograms of rat plasma drawn at different intervals after intravenous injection of [^{11}C]SA4503: A) 5 min, B) 10 min, C) 20 min, D) 40 min and E) 60 min.*

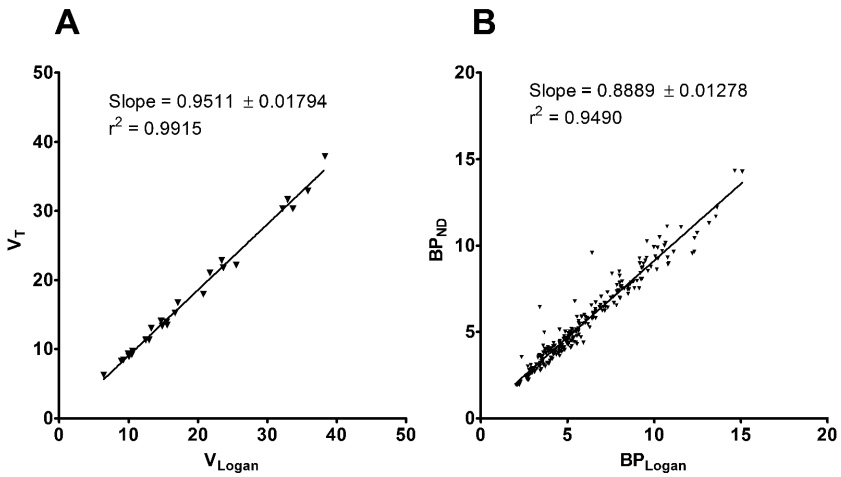

Supplementary Figure 4. *Comparison of data from 2-TCM and Logan graphical analysis. A) whole brain V_T, B) BP_{ND} of individual brain regions*

Supplementary Table 1. Additional animal data (body and brain weights, injected tracer dose and mass, input functions used for modeling)

Age group	1.5 months	3 months	18 months	24 months	32 months
Number of rats scanned	5	7	3	4	3
Number of rats used for metabolite analysis	4	3	2 (also scanned)	-	2 (also scanned)
Additional rats with pituitary tumor used only for metabolite analysis	-	-	1	-	3
Total number of brain TACs used for kinetic analysis	5	7	5	4	5
Number of rats where plasma data was not available and group averages were used	-	-	1 + (2 from metabolite analysis)	2	1 + (2 from metabolite analysis)
Number of rats where individual plasma data was available	5	7	2	2	2
Body weight in gram ± SEM	214.8 ± 3.3	307.7± 8.3	608.5± 9.2	594.8± 20.1	612± 18.0
Brain weight in gram ± SEM	1.725 ± 0.03	1.900± 0.04	2.217 ± 0.05	2.110 ± 0.04	2.111 ± 0.04
^{11}C-SA4503 dose injected in MBq ± SEM	10.3± 1.8	19.0± 2.1	34.7± 3.9	9.2± 1.3	36.5± 4.6
Upper limit of injected tracer mass (nmol)	0.10 ± 0.02	0.19 ± 0.02	0.35 ± 0.04	0.09 ± 0.01	0.37 ± 0.05

Supplementary Table 2. Parameters of 2-TCM fit to whole brain TACs in all study groups.

Age group	1.5 months	3 months	18 months	24 months	32 months
K_1	4.734 ± 1.237	2.431 ± 0.3097	1.078 ± 0.149	1.392 ± 0.361	0.702 ± 0.093
k_2	2.133 ± 0.789	0.738 ± 0.131	0.388 ± 0.073	0.879 ± 0.215	0.349 ± 0.052
k_3	0.276 ± 0.063	0.238 ± 0.046	0.119 ± 0.007	0.223 ± 0.039	0.112 ± 0.018
k_4	0.032 ± 0.002	0.039 ± 0.006	0.032 ± 0.001	0.039 ± 0.002	0.033 ± 0.002
V_T	26.59 ± 3.61	25.49 ± 3.13	14.22 ± 0.51	10.25 ± 1.26	8.27 ± 0.87
BP_{ND}	8.670 ± 2.034	6.266 ± 0.927	3.768 ± 0.323	5.508 ± 0.726	3.388 ± 0.366
K_1/k_2	2.672 ± 0.376	3.683 ± 0.439	2.876 ± 0.231	1.578 ± 0.095	2.044 ± 0.186

REFERENCES

1. Hayashi T, Su TP. Sigma-1 receptors at galactosylceramide-enriched lipid microdomains regulate oligodendrocyte differentiation. *Proc Natl Acad Sci U S A*. 2004;101:14949-14954.
2. Maurice T. Cognitive effects of sigma-receptor ligands. In: Matsumoto RR, Bowen WD, Su TP, eds. *Sigma Receptors: Chemistry, Cell Biology and Clinical Implications.* New York: Springer; 2007:237.
3. Takebayashi M, Hayashi T, Su TP. A perspective on the new mechanism of antidepressants: Neuritogenesis through sigma-1 receptors. *Pharmacopsychiatry*. 2004;37 Suppl 3:S208-S213.
4. Tsai SY, Hayashi T, Su TP. Hippocampal dendritogenesis and associated anchoring of NMDA and AMPA receptors are controlled by sigma-1 receptors. *Int J Neuropsychopharmacol.* 2006;9:S213.
5. Maurice T, Lockhart BP. Neuroprotective and anti-amnesic potentials of sigma receptor ligands. *Prog Neuropsychopharmacol Biol Psychiatry*. 1997;21:69-102.
6. Hayashi T, Su TP. Sigma-1 receptor chaperones at the ER-mitochondrion interface regulate ca(2+) signaling and cell survival. *Cell*. 2007;131:596-610.
7. Patrick SL, Walker JM, Perkel JM, Lockwood M, Patrick RL. Increases in rat striatal extracellular dopamine and vacuous chewing produced by two sigma receptor ligands. *Eur J Pharmacol*. 1993;231:243-249.
8. Gudelsky GA. Effects of sigma receptor ligands on the extracellular concentration of dopamine in the striatum and prefrontal cortex of the rat. *Eur J Pharmacol*. 1995;286:223-228.
9. Kobayashi T, Matsuno K, Murai M, Mita S. Sigma 1 receptor subtype is involved in the facilitation of cortical dopaminergic transmission in the rat brain. *Neurochem Res*. 1997;22:1105-1109.
10. Junien JL, Roman FJ, Brunelle G, Pascaud X. JO1784, a novel sigma ligand, potentiates [3H]acetylcholine release from rat hippocampal slices. *Eur J Pharmacol*. 1991;200:343-345.
11. Matsuno K, Matsunaga K, Mita S. Increase of extracellular acetylcholine level in rat frontal cortex induced by (+)N-allylnormetazocine as measured by brain microdialysis. *Brain Res*. 1992;575:315-319.
12. Matsuno K, Matsunaga K, Senda T, Mita S. Increase in extracellular acetylcholine level by sigma ligands in rat frontal cortex. *J Pharmacol Exp Ther*. 1993;265:851-859.
13. Matsuno K, Senda T, Kobayashi T, Mita S. Involvement of sigma 1 receptor in (+)-N-allylnormetazocine- stimulated hippocampal cholinergic functions in rats. *Brain Res*. 1995;690:200-206.
14. Kobayashi T, Matsuno K, Nakata K, Mita S. Enhancement of acetylcholine release by SA4503, a novel sigma 1 receptor agonist, in the rat brain. *J Pharmacol Exp Ther*. 1996;279:106-113.
15. Meyer DA, Carta M, Partridge LD, Covey DF, Valenzuela CF. Neurosteroids enhance spontaneous glutamate release in hippocampal neurons - possible role of metabotropic sigma(1)-like receptors. *J Biol Chem*. 2002;277:28725-28732.
16. Dong LY, Cheng ZX, Fu YM, et al. Neurosteroid dehydroepiandrosterone sulfate enhances spontaneous glutamate release in rat prelimbic cortex through activation of dopamine D1 and sigma-1 receptor. *Neuropharmacology*. 2007;52:966-974.
17. Dong Y, Fu YM, Sun JL, Zhu YH, Sun FY, Zheng P. Neurosteroid enhances glutamate release in rat prelimbic cortex via activation of alpha1-adrenergic and sigma1 receptors. *Cell Mol Life Sci*. 2005;62:1003-1014.
18. Muller WE, Stoll S, Scheuer K, Meichelbock A. The function of the NMDA-receptor during normal brain aging. *J Neural Transm Suppl*. 1994;44:145-158.
19. Smith TD, Gallagher M, Leslie FM. Cholinergic binding sites in rat brain: Analysis by age and cognitive status. *Neurobiol Aging*. 1995;16:161-173.

20. Giardino L. Right-left asymmetry of D1- and D2-receptor density is lost in the basal ganglia of old rats. *Brain Res*. 1996;720:235-238.

21. Meng SZ, Ozawa Y, Itoh M, Takashima S. Developmental and age-related changes of dopamine transporter, and dopamine D1 and D2 receptors in human basal ganglia. *Brain Res*. 1999;843:136-144.

22. Dewey SL, Volkow ND, Logan J, et al. Age-related decreases in muscarinic cholinergic receptor binding in the human brain measured with positron emission tomography (PET). *J Neurosci Res*. 1990;27:569-575.

23. Norbury R, Travis MJ, Erlandsson K, et al. In vivo imaging of muscarinic receptors in the aging female brain with (R,R)[123I]-I-QNB and single photon emission tomography. *Exp Gerontol*. 2005;40:137-145.

24. Maurice T, Urani A, Phan VL, Romieu P. The interaction between neuroactive steroids and the sigma1 receptor function: Behavioral consequences and therapeutic opportunities. *Brain Res Brain Res Rev*. 2001;37:116-132.

25. Phan VL, Miyamoto Y, Nabeshima T, Maurice T. Age-related expression of sigma1 receptors and antidepressant efficacy of a selective agonist in the senescence-accelerated (SAM) mouse. *J Neurosci Res*. 2005;79:561-572.

26. Wallace DR, Mactutus CF, Booze RM. Sigma binding sites identified by [(3)H] DTG are elevated in aged fischer-344 x brown norway (F1) rats. *Synapse*. 2000;35:311-313.

27. Ishiwata K, Kobayashi T, Kawamura K, Matsuno K. Age-related changes of the binding of [3h]SA4503 to sigma1 receptors in the rat brain. *Ann Nucl Med*. 2003;17:73-77.

28. Kawamura K, Kimura Y, Tsukada H, et al. An increase of sigma receptors in the aged monkey brain. *Neurobiol Aging*. 2003;24:745-752.

29. Majewska MD, Parameswaran S, Vu T, London ED. Divergent ontogeny of sigma and phencyclidine binding sites in the rat brain. *Brain Res Dev Brain Res*. 1989;47:13-18.

30. Matsumoto RR, Bowen WD, Walker JM. Age-related differences in the sensitivity of rats to a selective sigma ligand. *Brain Res*. 1989;504:145-148.

31. Paleos GA, Yang ZW, Byrd JC. Ontogeny of PCP and sigma receptors in rat brain. *Brain Res Dev Brain Res*. 1990;51:147-152.

32. Toyohara J, Sakata M, Ishiwata K. Imaging of sigma1 receptors in the human brain using PET and [11C]SA4503. *Cent Nerv Syst Agents Med Chem*. 2009;9:190-196.

33. Kawamura K, Elsinga PH, Kobayashi T, et al. Synthesis and evaluation of 11C- and 18F-labeled 1-[2-(4-alkoxy-3-methoxyphenyl)ethyl]-4-(3-phenylpropyl)piperazines as sigma receptor ligands for positron emission tomography studies. *Nucl Med Biol*. 2003;30:273-284.

34. Ramakrishnan NK, Rybczynska AA, Visser AK, et al. Small-animal PET with a sigma-ligand, 11C-SA4503, detects spontaneous pituitary tumors in aged rats. *J Nucl Med*. 2013;54:1377-1383.

35. Sakata M, Kimura Y, Naganawa M, et al. Mapping of human cerebral sigma1 receptors using positron emission tomography and [11C]SA4503. *Neuroimage*. 2007;35:1-8.

36. Ramakrishnan NK, Visser AK, Schepers M, et al. Dose-dependent sigma-1 receptor occupancy by donepezil in rat brain can be assessed with C-SA4503 and microPET. *Psychopharmacology (Berl)*. 2014.

37. Schweinhardt P, Fransson P, Olson L, Spenger C, Andersson JL. A template for spatial normalisation of MR images of the rat brain. *J Neurosci Methods*. 2003;129:105-113.

38. Julien-Dolbec C, Tropres I, Montigon O, et al. Regional response of cerebral blood volume to graded hypoxic hypoxia in rat brain. *Br J Anaesth*. 2002;89:287-293.

39. Brown WR, Thore CR. Review: Cerebral microvascular pathology in ageing and neurodegeneration. *Neuropathol Appl Neurobiol*. 2011;37:56-74.

40. Farrall AJ, Wardlaw JM. Blood-brain barrier: Ageing and microvascular disease--systematic review and meta-analysis. *Neurobiol Aging*. 2009;30:337-352.

41. Hedskog L, Pinho CM, Filadi R, et al. Modulation of the endoplasmic reticulum-mitochondria interface in alzheimer's disease and related models. *Proc Natl Acad Sci U S A*. 2013;110:7916-7921.